

# Epitope Mapping of Antibodies to the C-Terminal Region of the Integrin $\beta_2$ Subunit Reveals Regions that Become Exposed Upon Receptor Activation<sup>1</sup>

Chafen Lu,<sup>2</sup> Mazen Ferzly, Junichi Takagi, and Timothy A. Springer<sup>3</sup>

The cysteine-rich repeats in the stalk region of integrin  $\beta$  subunits appear to convey signals impinging on the cytoplasmic domains to the ligand-binding headpiece of integrins. We have examined the functional properties of mAbs to the stalk region and mapped their epitopes, providing a structure-function map. Among a panel of 14 mAbs to the  $\beta_2$  subunit, one, KIM127, preferentially bound to  $\alpha_L\beta_2$  that was activated by mutations in the cytoplasmic domains, and by  $Mn^{2+}$ . KIM127 also bound preferentially to the free  $\beta_2$  subunit compared with resting  $\alpha_L\beta_2$ . Activating  $\beta_2$  mutations also greatly enhanced binding of KIM127 to integrins  $\alpha_M\beta_2$  and  $\alpha_X\beta_2$ . Thus, the KIM127 epitope is shielded by the  $\alpha$  subunit, and becomes reexposed upon receptor activation. Three other mAbs, CBR LFA-1/2, MEM48, and KIM185, activated  $\alpha_L\beta_2$  and bound equally well to resting and activated  $\alpha_L\beta_2$ , differentially recognized resting  $\alpha_M\beta_2$  and  $\alpha_X\beta_2$ , and bound fully to activated  $\alpha_M\beta_2$  and  $\alpha_X\beta_2$ . The KIM127 epitope localizes within cysteine-rich repeat 2, to residues 504, 506, and 508. By contrast, the two activating mAbs CBR LFA-1/2 and MEM48 bind to overlapping epitopes involving residues 534, 536, 541, 543, and 546 in cysteine-rich repeat 3, and the activating mAb KIM185 maps near the end of cysteine-rich repeat 4. The nonactivating mAbs, 6.7 and CBR LFA-1/7, map more N-terminal, to subregions 344–432 and 432–487, respectively. We thus define five different  $\beta_2$  stalk subregions, mAb binding to which correlates with effect on activation, and define regions in an interface that becomes exposed upon integrin activation. *The Journal of Immunology*, 2001, 166: 5629–5637.

Lymphocyte function-associated Ag-1 (LFA-1,  $\alpha_L\beta_2$ , CD11a/CD18) is one of four integrins that are restricted in expression to leukocytes and have different  $\alpha$  subunits associated with a common integrin  $\beta_2$  subunit in  $\alpha\beta$  heterodimers (1–3). LFA-1 is expressed on all leukocytes, and is important in essentially all cell-cell interactions by immune cells, including Ag-specific interactions and binding of leukocytes in the circulation to the endothelium. The counterreceptors for LFA-1 are ICAMs that are members of the Ig superfamily. Other leukocyte integrins include  $\alpha_M\beta_2$  and  $\alpha_X\beta_2$ , which are primarily expressed on myeloid lineage cells and bind ligands including ICAM-1, the complement component iC3b, and fibrinogen. In common with many other integrins, the leukocyte or  $\beta_2$  integrins must be activated before they bind ligands, through a process termed inside-out signaling. For example, Ag recognition by receptors linked to tyrosine kinases, or recognition of chemoattractants by G protein-coupled receptors, activates intracellular signaling pathways that in turn activate adhesiveness through LFA-1 on a timescale of less than 1 s. In this way, LFA-1 acts as an adhesion servomotor under the control of other cell surface receptors, enabling dynamic modulation of cellular adhesion and migration.

A key question of current integrin research is how inside-out signals are transduced from the cytoplasm to the ligand-binding

domains, despite the presence of long  $\alpha$  and  $\beta$  subunit stalk regions that intervene between the transmembrane domains and the ligand-binding headpiece. Electron microscopy of integrins reveals an overall structure with a globular headpiece connected to the plasma membrane by two long stalks each  $\sim 16$  nm long (4). The headpiece binds ligand and contains domains from the N-terminal portions of both the  $\alpha$  and  $\beta$  subunits. The N-terminal region of the integrin  $\alpha$  subunits contains seven repeats of  $\sim 60$  aa each, and has been predicted to fold into a seven-bladed  $\beta$ -propeller domain (5) containing  $Ca^{2+}$ -binding  $\beta$ -hairpin loop motifs (6). About one-half of the integrin  $\alpha$  subunits, including the  $\alpha_L$ ,  $\alpha_M$ , and  $\alpha_X$  subunits, contain a domain of  $\sim 200$  aa that is inserted between  $\beta$ -sheets 2 and 3 of the  $\beta$ -propeller domain, and is termed the inserted (I) domain. The I domain has a structure similar to small G proteins, with a metal ion-dependent adhesion site (MIDAS)<sup>4</sup> at the top of the domain in which ligand is bound (7, 8). A conformational change at the MIDAS that regulates ligand binding is linked structurally to a large movement of the C-terminal  $\alpha$ -helix, which connects the bottom of the I domain to the  $\beta$ -propeller domain (8–12). Integrin  $\beta$  subunits contain an evolutionarily well-conserved domain of  $\sim 250$  residues in their N-terminal portion that has been predicted to have an I domain-like fold, and a MIDAS-like site (7, 13–16). This  $\beta$  subunit I-like domain associates with the side of the  $\alpha$  subunit  $\beta$ -propeller domain at  $\beta$ -sheets 2 and 3 (17, 18), and is thus near to the  $\alpha$  subunit I domain that links to  $\beta$ -sheets 2 and 3 at the top of the  $\beta$ -propeller domain.

The stalk regions provide the crucial link between signals impinging on the  $\alpha$  and  $\beta$  subunit transmembrane and cytoplasmic domains and the conformational changes that occur in the ligand-binding headpiece. In the  $\alpha$  subunit, the stalk region appears to consist of the region C-terminal to the predicted  $\beta$ -propeller domain, and contains  $\sim 500$  residues. Four subregions of the  $\alpha_M$  stalk

Center for Blood Research, Department of Pathology, Harvard Medical School, Boston, MA 02115

Received for publication November 11, 2000. Accepted for publication February 5, 2001.

The costs of publication of this article were defrayed in part by the payment of page charges. This article must therefore be hereby marked *advertisement* in accordance with 18 U.S.C. Section 1734 solely to indicate this fact.

<sup>1</sup> This work was supported by National Institutes of Health Grant CA31798. C.L. was supported by a fellowship from the Cancer Research Institute.

<sup>2</sup> Current address: Millennium Pharmaceuticals, 75 Sidney Street, Cambridge, MA 02139.

<sup>3</sup> Address correspondence and reprint requests to Dr. Timothy A. Springer, Department of Pathology, Center for Blood Research, Harvard Medical School, 200 Longwood Avenue, Room 251, Boston, MA 02115.

<sup>4</sup> Abbreviations used in this paper: MIDAS, metal ion-dependent adhesion site; PSI, plexins, semaphorins, and integrins.

region have been defined with mAb epitopes, three of which react with mAb whether or not the  $\beta$  subunit is coexpressed. The  $\alpha$  stalk region is predicted to consist of domains with a two-layer  $\beta$ -sandwich structure (19). In the  $\beta$  subunit, the stalk region appears to consist of regions that precede and follow the I-like domain; i.e., residues 1–103 and 342–678 in  $\beta_2$ . These regions include segments that are cysteine rich, and are linked by a long-range disulfide bond defined in  $\beta_3$  that is predicted to link Cys<sup>3</sup> and Cys<sup>425</sup> in  $\beta_2$  (20). The N-terminal cysteine-rich region of about residues 1–50 shares sequence homology with membrane proteins including plexins, semaphorins, and the *c-met* receptor (21). This region has two predicted  $\alpha$ -helices, and has been termed the PSI domain for plexins, semaphorins, and integrins. The region from residues 425 to 590 has a high cysteine content (20%), and is composed of four repeats. The first repeat is less similar to the others, and at its N-terminal end contains the cysteine that disulfide bonds to the PSI domain.

The  $\beta$  subunit stalk region appears to be important for regulating ligand binding in the headpiece. Several Abs that activate integrins or bind to activated forms of integrins have been mapped to these regions. The mAb LIBS2, which increases the affinity of the platelet integrin  $\alpha_{IIb}\beta_3$  for fibrinogen, maps to an 89-aa region next to the transmembrane region (22). The mAb TASC promotes cell adhesion to laminin, and binds to the region from residues 493 to 602 in the chicken  $\beta_1$  subunit (23). Another  $\beta_1$  integrin-activating mAb, QE.2E5, binds to the  $\beta_1$  cysteine-rich repeats (24). mAb 9EG7 recognizes a  $\beta_1$  subunit epitope between residues 495 and 602 that becomes exposed after activation of  $\beta_1$  integrins, and activates ligand binding by multiple  $\beta_1$  integrins (25). Similarly, mAb AG89, which maps to residues 426–587 in the  $\beta_1$  subunit, recognizes an epitope that becomes exposed after activation of  $\beta_1$  integrins (26). Four activating mAbs to the  $\beta_2$  subunit, KIM127, KIM185, CBR LFA-1/2, and MEM48 (27–30), bind to the  $\beta_2$  cysteine-rich region (18, 31). Thus, structural changes in the stalk region that include exposing Ab epitopes on the integrin  $\beta$  subunit are associated with integrin activation. However, the location of these  $\beta$  subunit epitopes has not been narrowed to specific cysteine-rich repeats, e.g., residues 406–570 to which KIM127 maps include repeats 1, 2, 3, and 4 (31). In many cases, the epitopes have been mapped not to the cysteine-rich repeats themselves, but to regions that include the cysteine-rich repeats and adjacent N-terminal or C-terminal segments.

In this study, we define specific amino acid residues and domains in the integrin  $\beta_2$  stalk region that are exposed during activation, and to which activating Abs bind. We demonstrate that mAb KIM127 preferentially reacts with activated  $\beta_2$  integrins and the free  $\beta_2$  subunit compared with resting  $\beta_2$  integrins. We also demonstrate differences between resting  $\alpha_L\beta_2$ ,  $\alpha_M\beta_2$ , and  $\alpha_X\beta_2$  in the exposure of the CBR LFA-1/2, KIM185, and MEM48 epitopes on the  $\beta_2$  stalk. We map the epitopes of these four activating mAbs, and the epitopes of two mAbs that are not activating. KIM127 recognizes residues 504, 506, and 508 in cysteine-rich repeat 2, two activating mAbs recognize three to five residues in cysteine-rich repeat 3, and another activating mAb binds near the end of cysteine-rich repeat 4. By contrast, two nonactivating mAbs bind to subregions between the I-like domain and the region to which activating mAbs bind. We thus provide a structure-function map for the  $\beta_2$  stalk region, and identify residues in interfaces that become exposed upon integrin activation.

## Materials and Methods

### Monoclonal Abs

The murine mAbs TS1/18, CBR LFA-1/7, and CBR LFA-1/2 to human  $\beta_2$  (CD18) were described previously (30, 32). The mAbs KIM127 (27) and KIM185 (28) were kindly provided by M. Robinson (Celltech, Berkshire,

U.K.). MEM48 (33) was generously provided by V. Horejshi (Institute of Molecular Genetics, Prague, Czechoslovakia). YFC51 and YFC118 (34) were kindly donated by G. Hale (University of Oxford, Oxford, U.K.). The mAbs 6.7 (35), GRF1 (36), CLB54 (37), and CLBLFA-1/1 (38) were obtained from the Fifth International Leukocyte Workshop. The murine mAbs TS1/22 and TS2/4 to human  $\alpha_L$ , and the myeloma IgG1 X63 were described previously (32).

### Cell lines

Human embryonic kidney 293T cells were cultured in DMEM supplemented with 10% FBS, 2 mM glutamine, and 50  $\mu$ g/ml gentamicin. JY cells (human B lymphoblastoid cell line) were cultured in RPMI 1640/10% FBS, 50  $\mu$ g/ml gentamicin. Jurkat- $\beta_2.7$  (J $\beta_2.7$ ) transfectants and K562 transfectants that express wild-type or mutant LFA-1 were described previously (39), and cultured in RPMI 1640/10% FBS supplemented with 4  $\mu$ g/ml puromycin.

### Construction of $\beta_2$ mutants

The wild-type human and mouse  $\beta_2$  subunit cDNAs were contained in the expression vector AprM8, a derivative of CDM8 (40). Chimeric human and mouse  $\beta_2$  subunits were generated by overlap extension PCR (41, 42). For making chimeras with mouse sequence at the N-terminal portion and human sequence at the C-terminal portion, outer left and outer right primers for overlap PCR were used that were designated mEcoRV and hNOTI, respectively. mEcoRV was 5' to the EcoRV site at nucleotide 310 in the mouse  $\beta_2$  cDNA, and hNOT I was 3' to the stop codon of the human  $\beta_2$  cDNA, and contained a stop codon, a *NheI* recognition sequence, and a *NotI* site. The inner primers designed for each individual chimera contained overlapping sequences. The first PCRs used the mouse and human  $\beta_2$  cDNA to amplify the mouse and human sequences, respectively. The second PCR product was digested with EcoRV and *NotI*, and the 2.1-kb EcoRV-*NotI* fragment was swapped into the same sites in the wild-type mouse  $\beta_2$  cDNA. The unique *NheI* site was used for mutant identification. A similar approach was used to make chimeras with the N-terminal portion of human sequence and C-terminal mouse sequence. Briefly, the outer left PCR primer, hBsrG, was 5' to the BsrG I site at nucleotide 947 of the human  $\beta_2$  cDNA, and the outer right primer, mNot I, was complementary to the mouse  $\beta_2$  cDNA, and contained a stop codon followed by a *NheI* site and a *NotI* site. The second PCR product was cut with BsrG I and *NotI*, and the 1.4-kb BsrG I and *NotI* fragment was swapped into the wild-type human  $\beta_2$  cDNA at the same sites. Overlap extension PCR was also used to make human to mouse amino acid substitution mutants. The outer left and right PCR primers were hBsrG and hNOT I, respectively. The inner PCR primers were designed to contain the desired mutations. The second PCR product was cut with BsrG I and *NotI*, and swapped into the wild-type human  $\beta_2$  cDNA at the same sites. All mutations were confirmed by DNA sequencing.

### Transient transfection of 293T cells

The 293T cells were transfected using the calcium phosphate precipitate method (43, 44). Briefly, 7.5  $\mu$ g wild-type or mutant  $\beta_2$  cDNA and 7.5  $\mu$ g  $\alpha_L$  cDNA were used to cotransfect one 6-cm plate of 70–80% confluent cells. Two days after transfection, cells were detached from the plate with HBSS containing 5 mM EDTA and washed twice for flow cytometric analysis.

### Flow cytometry

Cells were harvested and washed twice with L15 medium (Sigma, St. Louis, MO) containing 2.5% FBS (L15/FBS). Cells ( $10^5$ ) were incubated with primary Ab in 100  $\mu$ l L15/FBS on ice for 30 min, except for KIM127. Incubation with mAb KIM127 was conducted at 37°C for 30 min (27). The mAbs TS1/18, CBR LFA-1/7, CBR LFA-1/2, KIM127, KIM185, MEM48, YFC51, YFC118, TS1/22, and TS2/4 were used as purified IgG at 15  $\mu$ g/ml, and the International Leukocyte Workshops mAbs 6.7, GRF, CLBLFA-1/1, and CLB54 were used at 1/100 dilution. The control IgG X63 was used as 1/5 dilution of hybridoma supernatant. Cells were then washed twice with L15/FBS and incubated with FITC-conjugated goat anti-mouse IgG (heavy and light chain; Zymed Laboratories, San Francisco, CA) for 30 min on ice. After washing, cells were resuspended in cold PBS and analyzed on a FACScan (BD Biosciences, San Jose, CA).

### Cell adhesion

Cell adhesion to purified ICAM-1 was described previously (39). Briefly, cells were labeled with 2',7'-bis-(carboxyethyl)-5 (and -6)-carboxyfluorescein, acetoxymethyl ester, and resuspended to  $10^6$ /ml in L15/FBS. Cell suspensions (50  $\mu$ l) were mixed in ICAM-1-coated wells with an equal volume of L15/FBS containing activating or control mAb. After incubation

at 37°C for 30 min, unbound cells were washed off on a Microplate Autowasher (Biotek Instruments, Winooski, VT). The fluorescence content of total input cells and the bound cells in each well was quantitated on a Fluorescent Concentration Analyzer (Idexx, Westbrook, ME). The bound cells were expressed as a percentage of total input cells.

## Results

### *The mAb KIM127 preferentially binds to constitutively active $\alpha_L\beta_2$ mutants and the unassociated $\beta_2$ subunit*

The mAbs were tested for differential reactivity with mutationally activated and wild-type LFA-1.  $\alpha_L$  subunit mutations with a complete truncation of the cytoplasmic domain,  $\alpha_L1090^*$ , and an internal deletion of the conserved GFFKR motif in the cytoplasmic domain,  $\alpha_L\Delta GFFKR$ , activated binding to ICAM-1 of  $\alpha_L\beta_2$  heterodimers expressed in several cell types, including K562 cells and J $\beta_2.7$  cells (39). These mutants also express the activation-dependent m24 epitope (45). Of a panel of 14 mAbs to the  $\beta_2$  subunit, one mAb, KIM127, stained transfectants expressing wild-type  $\alpha_L\beta_2$  much more weakly than the other mAbs (Fig. 1). By contrast, KIM127 bound almost as well to the constitutively active  $\alpha_L\beta_2$  mutants as the other mAbs (Fig. 1). KIM127 mAb bound 7.5- and 5.3-fold better to  $\alpha_L1090^*$   $\beta_2$  and  $\alpha_L\Delta GFFKR$   $\beta_2$  complexes, respectively, than to wild-type  $\alpha_L\beta_2$  (Table I). By contrast, the other 13 mAbs to  $\beta_2$  bound equally well to wild-type  $\alpha_L\beta_2$  and the constitutively active mutants (Table I and Fig. 1). These included five other mAbs to the C-terminal region of  $\beta_2$ , mAbs 6.7, MEM48, CBR LFA-1/7, CBR LFA-1/2, and KIM185.

$\alpha_L\beta_2$  can also be activated by truncation of the  $\beta_2$  cytoplasmic domain, i.e., by mutation  $\beta_2702^*$  (46) (our unpublished data). Although KIM127 bound less well than other mAbs to 293T transfectants expressing wild-type  $\alpha_L\beta_2$ , it bound to  $\alpha_L\beta_2$  containing the  $\beta_2702^*$  mutation as well as other mAbs (Table II). In all cells examined that constitutively expressed LFA-1, including JY lymphocytes (see below), KIM127 mAb bound markedly less well than other Abs to  $\alpha_L\beta_2$ . Furthermore, in all transfectants examined, including J $\beta_2.7$  cells and K562 cells (see below), KIM127 bound less well than other Abs to wild-type  $\alpha_L\beta_2$ , and bound

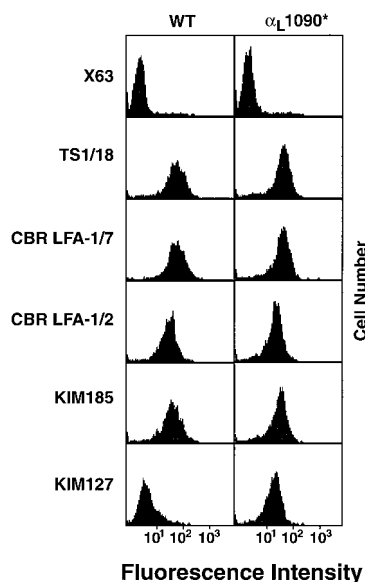


**FIGURE 1.** The mAb KIM127 preferentially binds to the constitutively active  $\alpha_L\beta_2$  mutant  $\alpha_L1090^*$ . J $\beta_2.7$  transfectants that express wild-type  $\alpha_L\beta_2$  or the  $\alpha_L\beta_2$  mutant  $\alpha_L1090^*$  were stained with the control myeloma X63 or the indicated mAb to the  $\beta_2$  subunit, then with FITC-conjugated anti-IgG, and subjected to immunofluorescent flow cytometry.

**Table I.** Reactivity of Abs with the constitutively active  $\alpha_L\beta_2$  mutants  $\alpha_L1090^*$  and  $\alpha_L\Delta GFFKR$ <sup>a</sup>

mAb	Binding (% of wild type)	
	$\alpha_L1090^*$	$\alpha_L\Delta GFFKR$
$\beta_2$ I-like domain		
GRF1	98 ± 5	81 ± 0
YFC51	95 ± 4	96 ± 2
YFC118.3	96 ± 3	93 ± 2
TS1/18	103 ± 5	88 ± 8
CLB54	106 ± 7	104 ± 6
CLBLFA1/1	120 ± 13	107 ± 7
6.5E	99 ± 3	94 ± 2
May.017	106 ± 7	94 ± 2
$\beta_2$ C-terminal region		
6.7	107 ± 4	105 ± 0
CBR LFA-1/7	94 ± 7	99 ± 3
KIM127	745 ± 56	526 ± 5
CBR LFA-1/2	105 ± 6	109 ± 7
MEM48	107 ± 11	108 ± 1
KIM185	114 ± 5	117 ± 3

<sup>a</sup> Reactivity of Abs with stable J $\beta_2.7$  transfectants that express wild-type or mutant  $\alpha_L\beta_2$  was determined by flow cytometry. Mean fluorescence of each Ab after subtraction of background binding was normalized to the mean fluorescence of mAb TS2/4. The mAb TS2/4 recognizes the  $\alpha_L$  subunit in  $\alpha_L\beta_2$  complex. Because of differences between transfectants in level of expression, the mean fluorescence of TS2/4 mAb after subtraction of background was 97 ± 11, 72 ± 5 and 137 ± 14 for wild type,  $\alpha_L1090^*$ , and  $\alpha_L\Delta GFFKR$ , respectively. Data shown are mean ± SD of three independent experiments.

markedly better to  $\alpha_L\beta_2$  containing activating mutations in the  $\alpha_L$  or  $\beta_2$  cytoplasmic domains. These results demonstrate that the KIM127 epitope is more exposed in mutationally activated  $\alpha_L\beta_2$  than in the resting, wild-type  $\alpha_L\beta_2$  molecule.

The  $\beta_2$  subunit can be expressed in the absence of integrin  $\alpha$  subunits in transfected cells, although with less efficiency than as an  $\alpha\beta$  complex (47). Therefore, we examined binding of KIM127 mAb to the  $\beta_2$  subunit expressed alone on the surface of 293T transfectants. KIM127 bound to  $\beta_2$  expressed in isolation from  $\alpha_L$  as well as the other mAbs to the  $\beta_2$  C-terminal region, 6.7, MEM48, CBR LFA-1/7, CBR LFA-1/2, and KIM185 (Table II). Thus, in resting, wild-type  $\alpha_L\beta_2$ , the KIM127 epitope is shielded by the  $\alpha_L$  subunit.

### *Induction of KIM127 epitope exposure by $Mn^{2+}$ and PMA*

$Mg^{2+}$  in the absence of  $Ca^{2+}$ , and  $Mn^{2+}$  have previously been reported to activate adhesiveness of LFA-1 (45, 48).  $Mn^{2+}$  greatly

**Table II.** Reactivity of Abs with  $\alpha_L\beta_2$ ,  $\alpha_L\beta_2$  activated with the  $\beta_2702^*$  mutation, or the  $\beta_2$  subunit expressed alone in 293T cells<sup>a</sup>

mAb	Binding (% of CBR LFA-1/7)		
	$\alpha_L + \beta_2$	$\alpha_L + \beta_2702^*$	$\beta_2$ alone
$\alpha_L$ subunit			
TS1/22	115 ± 3	99 ± 1	0 ± 0
$\beta_2$ C-terminal region			
6.7	106 ± 5	91 ± 1	109 ± 12
KIM127	14 ± 4	101 ± 8	107 ± 2
CBR LFA-1/2	90 ± 4	85 ± 3	91 ± 3
MEM48	90 ± 4	86 ± 5	92 ± 0
KIM185	85 ± 7	81 ± 3	91 ± 5

<sup>a</sup> The 293T cells were transiently transfected with wild-type  $\alpha_L$  and  $\beta_2$ , wild-type  $\alpha_L$  and  $\beta_2702^*$ , or  $\beta_2$  alone. Reactivity of Abs with the 293T transfectants was determined by immunofluorescence flow cytometry. Mean fluorescence of each Ab after subtraction of background binding was normalized to the mean fluorescence of mAb CBR LFA-1/7. The mAb CBR LFA-1/7 maps to the  $\beta_2$  C-terminal region and binds  $\alpha_L\beta_2$ ,  $\alpha_L\beta_2702^*$ , and  $\beta_2$  alone equally well. Data are presented as the mean ± difference from the mean of two independent experiments.



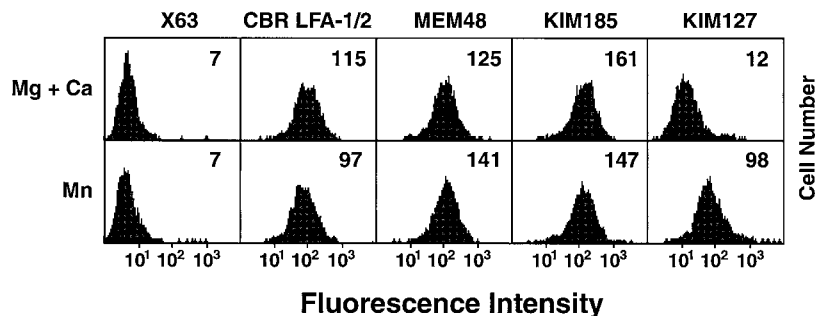


**FIGURE 2.**  $\text{Mn}^{2+}$  increases mAb KIM127 binding. K562 cells transfected with  $\alpha_L\beta_2$  were harvested and washed twice with 20 mM Tris (pH 7.5), 150 mM NaCl (TBS) containing 5 mM EDTA. After two washes with TBS without EDTA, cells were resuspended in TBS supplemented with 1 mM each of  $\text{Mg}^{2+}$  and  $\text{Ca}^{2+}$ , or with 1 mM  $\text{Mn}^{2+}$ , and incubated with myeloma X63 IgG or the indicated  $\beta_2$  mAbs. Cells were incubated with FITC-conjugated anti-IgG and subjected to immunofluorescent flow cytometry. Mean fluorescence intensity of mAb staining after subtraction of the mean fluorescence intensity of X63 staining is shown in the right corner of each histogram, except that the fluorescence intensity of X63 is shown before subtraction.

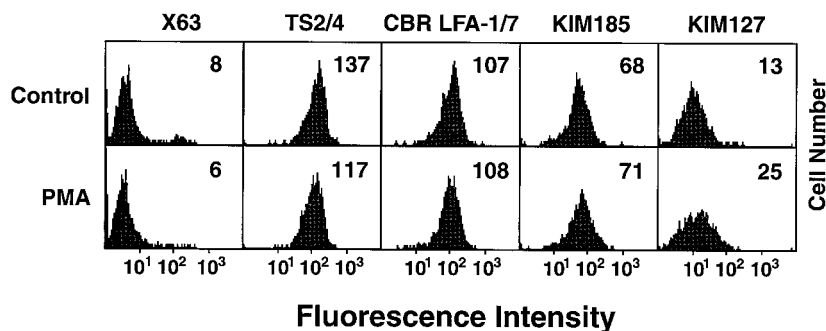
increased KIM127 binding to wild-type LFA-1 expressed on the surface of K562 transfectants, whereas binding of other  $\beta_2$  mAbs was not affected (Fig. 2). KIM127 binding was increased 8.3-fold in the presence of  $\text{Mn}^{2+}$ .  $\text{Mg}^{2+}$  in the absence of  $\text{Ca}^{2+}$  also increased KIM127 binding, but to a lesser degree than  $\text{Mn}^{2+}$  (data not shown). Similar results were obtained with JY cells (data not shown). Therefore, activation of LFA-1 ligand binding by  $\text{Mn}^{2+}$ , and  $\text{Mg}^{2+}$  in the absence of  $\text{Ca}^{2+}$ , correlates with increased expression of the KIM127 epitope.

Increased binding of LFA-1 to its ligand ICAM-1 can be induced by treatment of LFA-1-expressing cells with PMA (49, 50), although this may be a result of increased clustering on the cell surface rather than a change in affinity for ICAM-1 (51). PMA treatment of JY cells increased KIM127 binding by  $\sim 2$ -fold, whereas binding of other mAbs was unchanged (Fig. 3). Although this increase was consistently less than that seen with  $\text{Mn}^{2+}$ , it was significant and reproducible.

#### *KIM127 activates ligand binding by LFA-1 to a level similar to three other activating mAbs*

The mAbs KIM127, KIM185, CBR LFA-1/2, and MEM48 have all previously been reported to increase  $\alpha_L\beta_2$ -mediated cell adhesion and cell aggregation (27–30), but have not been compared with one another. We compared these mAbs for their ability to activate LFA-1-dependent binding to ICAM-1. K562 transfectants expressing wild-type  $\alpha_L\beta_2$  did not bind to ICAM-1 in the presence of the nonbinding control IgG X63 or mAbs 6.7 or CBR LFA-1/7 to the C-terminal region of  $\beta_2$  (Fig. 4). By contrast, KIM127, CBR LFA-1/2, MEM48, and KIM185 greatly increased binding of cells to ICAM-1. Furthermore, the four mAbs activated  $\alpha_L\beta_2$  binding to ICAM-1 to a similar level (Fig. 4). The four mAbs also activated  $\alpha_L\beta_2$  binding to ICAM-1 to a similar level in J $\beta_2$ .7 transfectants (data not shown).

**FIGURE 3.** Effect of PMA on mAb KIM127 binding. JY cells were incubated with the indicated Abs in the absence (control) or presence of 100 ng/ml PMA for 30 min at 37°C. After two washes, cells were stained with FITC-conjugated anti-IgG and subjected to immunofluorescent flow cytometry. X63, control myeloma IgG; TS2/4, mAb to  $\alpha_L$  in complex with  $\beta_2$ . Mean fluorescence intensity of mAb staining after subtraction of the mean fluorescence intensity of X63 staining is shown in the right corner of each histogram, except that the fluorescence intensity of X63 is shown before subtraction.



*KIM127 reacts weakly with resting  $\alpha_L\beta_2$ ,  $\alpha_M\beta_2$ , and  $\alpha_X\beta_2$ , whereas three other activating  $\beta_2$  mAbs bind differentially to these integrins*

We compared the reactivity of KIM127 and the three other  $\beta_2$ -activating mAbs for  $\alpha_L\beta_2$ ,  $\alpha_M\beta_2$ , and  $\alpha_X\beta_2$  (Table III). KIM127 reacted weakly with resting  $\alpha_L\beta_2$ ,  $\alpha_M\beta_2$ , and  $\alpha_X\beta_2$ , compared with mAb CBR LFA-1/7. By contrast, the activating  $\beta_2$ 702\* truncation induced KIM127 reactivity to the same level as mAb CBR LFA-1/7 for all three  $\alpha\beta$  complexes (Table III). The mAbs CBR LFA-1/2, MEM48, and KIM185 reacted with the three resting  $\alpha\beta$  complexes differentially. As described above, all three mAbs bound to  $\alpha_L\beta_2$  as well as CBR LFA-1/7. However, CBR LFA-1/2 showed markedly reduced binding to  $\alpha_M\beta_2$  and  $\alpha_X\beta_2$  (Table III). MEM48 showed weak binding to  $\alpha_X\beta_2$  and moderate binding to  $\alpha_M\beta_2$ , whereas KIM185 bound to  $\alpha_M\beta_2$  weakly. By contrast, binding of CBR LFA-1/2, MEM48, and KIM185 to  $\alpha_L\beta_2$ 702\*,  $\alpha_M\beta_2$ 702\*, and  $\alpha_X\beta_2$ 702\* was comparable with mAb CBR LFA-1/7. The results demonstrate that the KIM127 epitope is shielded in all three  $\beta_2$  integrins in the resting state, and that epitopes of CBR LFA-1/2, MEM48, and KIM185 are differentially exposed in resting  $\alpha_L\beta_2$ ,  $\alpha_M\beta_2$ , and  $\alpha_X\beta_2$ . Differences in shielding may reflect differences in the structures of the  $\alpha_L$ ,  $\alpha_M$ , and  $\alpha_X$  subunits.

#### *Epitope mapping of mAb KIM127 and five other mAbs to the C-terminal region of the $\beta_2$ subunit*

To understand the molecular basis of  $\alpha_L\beta_2$  activation, we mapped the epitopes of KIM127, MEM48, CBR LFA-1/2, and KIM185. For comparison, we also mapped two nonactivating mAbs, 6.7 and CBR LFA-1/7. These mAbs had previously been shown to bind within a segment in the  $\beta_2$  subunit lying between the I-like domain and the transmembrane domain (15, 16, 31). A series of human and mouse chimeric  $\beta_2$  subunits were constructed. In these  $\beta_2$  chimeras, a segment of the human sequence in the region from residues

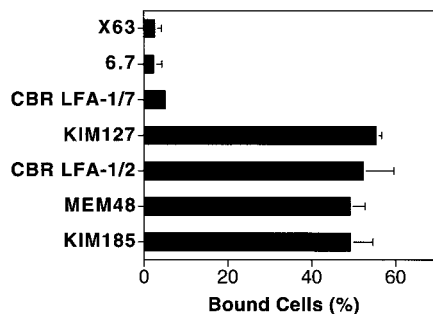


**FIGURE 4.** The mAbs KIM127, CBR LFA-1/2, MEM48, and KIM185 activate binding of  $\alpha_L\beta_2$ -expressing K562 cells to ICAM-1. ICAM-1 was coated at 250 ng/well overnight at 4°C. Binding of K562 transfectants that express wild-type  $\alpha_L\beta_2$  to immobilized ICAM-1 was performed in the presence of the control myeloma IgG X63 or the indicated mAb to the  $\beta_2$  subunit at 10  $\mu$ g/ml. Results are mean  $\pm$  SD of triplicate samples and are representative of two independent experiments.

344–621 was progressively replaced by the corresponding mouse sequence (Fig. 5). Reciprocal exchanges were also made in which mouse sequence was progressively replaced with human sequence. The chimeric  $\beta_2$  subunits were coexpressed with the human  $\alpha_L$  subunit in 293T cells, and mAb reactivity with the  $\alpha_L\beta_2$  complex was determined by immunofluorescence flow cytometry. All  $\beta_2$  chimeras were expressed on the cell surface at levels comparable with that of human  $\beta_2$ . The overall results are summarized in Table IV, and raw immunofluorescence flow cytometry data are shown for the mutants that were key for mapping KIM127 (Fig. 6). Although KIM127 bound less well to  $\alpha_L\beta_2$  in 293T transfectants than other mAbs, such as the positive control mAb TS1/18 to  $\beta_2$ , the reactivity of KIM127 was far above background, allowing mutations that abolished its binding to be easily identified (Fig. 6). The epitopes of the six mAbs localized to five different subregions, residues 344–432 (mAb 6.7), residues 432–487 (mAb CBR LFA-1/7), residues 487–538 (mAbs KIM127 and CBR LFA-1/2), residues 487–581 (mAb MEM48), and residues 581–621 (mAb KIM185) (Table IV).

Individual mouse-human amino acid substitutions were made in the region from residues 478–581 to define the epitopes of mAbs KIM127, CBR LFA-1/2, and MEM48. This region contains 23 aa that differ between the human and mouse  $\beta_2$  sequences (Fig. 7). First, this region was divided into 10 subregions that contained either one amino acid substitution, or two or three nearby amino acid substitutions. These 10 mutants were tested for effect on Ab

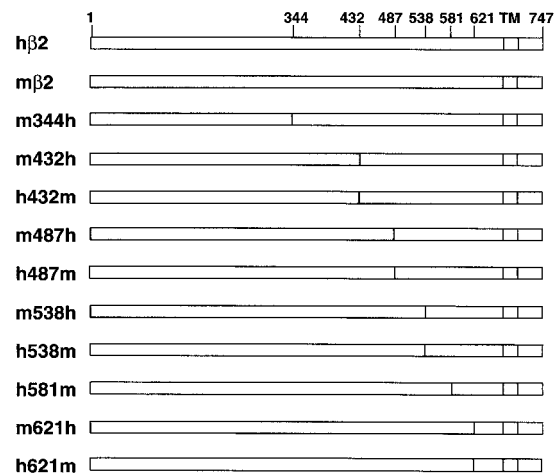


**FIGURE 5.** Schematic diagram of the human-mouse chimeric  $\beta_2$  subunits. Amino acid residues at the boundaries between human and mouse sequences are indicated above the human  $\beta_2$  subunit. Abbreviations used: h $\beta_2$ , human  $\beta_2$ ; m $\beta_2$ , mouse  $\beta_2$ ; TM, transmembrane domain.

binding. Subsequently, single amino acid substitutions were made within any region containing two or three substitutions that was found to affect mAb binding.

Results from the two rounds of mutagenesis are summarized in Table V. mAb KIM127 binding localized to residues 504, 506, and 508. The mutation G504N/L506E/Y508F completely abolished binding, while substitutions in the other subregions had no effect. The three individual amino acid substitutions G504N, L506E, and Y508F each partially reduced binding of mAb KIM127, with G504N (Gly→Asn) having the largest effect.

Binding of mAb MEM48 was completely eliminated by the substitutions L534S/F536N and R541S/H543K/F536Y, and unaffected by substitutions in other subregions. The single substitutions L534S and F536N both reduced MEM48 binding to 25% of wild type. Substitution H543K completely abolished MEM48 binding, whereas substitutions R541S and F536Y had no effect. Thus, MEM48 binding requires residues Leu<sup>534</sup>, Phe<sup>536</sup>, and His<sup>543</sup>.

The mAb CBR LFA-1/2 mapped to a set of residues overlapping with the MEM48 epitope. Binding of mAb CBR LFA-1/2 was abolished by mutation L534S/F536N and reduced to 40% of wild type by mutation R541S/H543K/F546Y. The single substitution F536N reduced CBR LFA-1/2 binding to 40% of wild type, whereas the single substitution L534S had no effect. Although the

Table III. Differential reactivity of activating anti- $\beta_2$  mAb with  $\alpha_L\beta_2$ ,  $\alpha_M\beta_2$ , and  $\alpha_X\beta_2$ <sup>a</sup>

	Binding (% CBR LFA-1/7)					
	$\alpha_L\beta_2$	$\alpha_L\beta_2$ 702*	$\alpha_M\beta_2$	$\alpha_M\beta_2$ 702*	$\alpha_X\beta_2$	$\alpha_X\beta_2$ 702*
mAb						
KIM127	14 $\pm$ 4	101 $\pm$ 8	10 $\pm$ 7	91 $\pm$ 3	16 $\pm$ 2	99 $\pm$ 2
CBR LFA-1/2	90 $\pm$ 4	85 $\pm$ 3	18 $\pm$ 5	87 $\pm$ 7	7 $\pm$ 2	80 $\pm$ 2
MEM48	90 $\pm$ 4	85 $\pm$ 3	61 $\pm$ 9	87 $\pm$ 7	13 $\pm$ 1	91 $\pm$ 3
KIM185	85 $\pm$ 7	81 $\pm$ 3	9 $\pm$ 7	92 $\pm$ 10	74 $\pm$ 0	86 $\pm$ 2
CBRM1/5 (to $\alpha_M$ )	ND	ND	20 $\pm$ 1	112 $\pm$ 5	ND	ND

<sup>a</sup> The 293T cells were transiently transfected with wild-type  $\alpha_L$ ,  $\alpha_M$ , or  $\alpha_X$  together with either wild-type  $\beta_2$  or the  $\beta_2$  mutant  $\beta_2$ 702\*.  $\alpha_M\beta_2$  and  $\alpha_M\beta_2$ 702\* were also stably expressed in K562 cells. Reactivity of Abs with the 293T and K562 transfectants was determined by immunofluorescence flow cytometry. Mean fluorescence of each Ab after subtraction of background binding was normalized to the mean fluorescence of mAb CBR LFA-1/7. The mAb CBR LFA-1/7 binds the wild-type  $\alpha_L\beta_2$  and mutant  $\alpha_L\beta_2$ 702\* heterodimers equally well. CBRM1/5 binds to an activation epitope in the  $\alpha_M$  I domain (10). Data are presented as the mean  $\pm$  difference from the mean of two independent experiments with 293T transfectants for  $\alpha_L\beta_2$ ,  $\alpha_L\beta_2$ 702\*,  $\alpha_X\beta_2$ , and  $\alpha_X\beta_2$ 702\*. For  $\alpha_M\beta_2$  and  $\alpha_M\beta_2$ 702\*, data are presented as the mean  $\pm$  SD from two experiments with K562 transfectants and one experiment with 293T transfectants.

Table IV. Monoclonal Ab reactivity with chimeric human-mouse  $\beta_2$  subunits expressed with human  $\alpha_L$ <sup>a</sup>

$\beta_2$ chimera	6.7	CBR LFA-1/7	KIM127	CBR LFA-1/2	MEM48	KIM185
m344h	+	+	+	+	+	+
m432h	—	+	+	+	+	+
h432m	+	—	—	—	—	—
m487h	—	—	+	+	+	+
h487m	+	+	—	—	—	—
m538h	—	—	—	—	—	+
h538m	+	+	+	+	—	—
h581m	+	+	+	+	+	—
m621h	—	—	—	—	—	—
h621m	+	+	+	+	+	+
epitope	344–432	432–487	487–538	487–538	487–581	581–621

<sup>a</sup> Human-mouse chimeric  $\beta_2$  was expressed in 293T cells in association with human  $\alpha_L$ . The mAb reactivity was determined by flow cytometry of the transfected cells. +, Positive staining with mean fluorescence intensity comparable to wild-type human  $\beta_2$ ; —, staining was not significantly different from mock-transfected 293T cells stained with the same mAb.

L534S substitution had no effect on its own, it synergized with F536N, because the L534S/F536N mutation had a more severe effect on CBR LFA-1/2 binding than the F536N mutation. Although the mutation R541S/H543K/F546Y reduced CBR LFA-1/2 binding, individual substitutions at residues 541, 543, and 546 had no effect. Therefore, the CBR LFA-1/2 epitope includes residues Phe<sup>536</sup> and to a lesser extent Leu<sup>534</sup>, and some combination of residues Arg<sup>541</sup>, His<sup>543</sup>, and Phe<sup>546</sup>.

Discussion

The stalk region of integrin  $\beta$  subunits appears to have an important function in inside-out signaling. The stalk region conveys signals that impinge on integrin cytoplasmic domains to the ligand-binding integrin headpiece. For the first time, we have mapped Abs

to specific amino acid residues and specific cysteine-rich repeats in this region of integrin  $\beta$  subunits. Previously, certain Abs to integrin  $\beta$  subunits have been reported to either activate ligand binding by integrins, or to bind in a manner that is dependent on integrin activation or binding to ligand. We have directly compared four such Abs to the integrin  $\beta_2$  subunit.

The original report on mAb KIM127 showed that it bound to the integrin  $\beta_2$  subunit and promoted LFA-1- and Mac-1-mediated cell-adhesive events (27). We found that KIM127 bound weakly to wild-type  $\alpha_L\beta_2$  on the surface of JY cells, and a number of  $\alpha_L\beta_2$ -transfected cell lines, including J $\beta$ 2.7 cells, 293T, and K562 cells. The level of KIM127 binding to wild-type  $\alpha_L\beta_2$  was only 10–15% of that found with other  $\beta_2$  mAbs. However, KIM127 binding to the same cells transfected with constitutively active  $\alpha_L\beta_2$  bearing  $\alpha_L$ 1090\*,  $\alpha_L$  $\Delta$ GFFKR, or  $\beta_2$ 702\* mutations was greatly increased, to the same level as seen for typical mAb to the  $\beta_2$  and  $\alpha_L$  subunits. These  $\alpha_L\beta_2$  mutants constitutively bind to ICAM-1, and express the activation epitope defined by the m24 mAb (39 and our unpublished data). Although increased exposure of the KIM127 epitope correlates with the expression of the m24 epitope, KIM127 differs from m24 in its ability to activate  $\beta_2$  integrins. Furthermore, mAb m24 differs from the mAbs investigated in this study, because it maps to the I-like domain of  $\beta_2$  (58). Binding of mAb KIM127 to wild-type  $\alpha_L\beta_2$  was greatly increased in the presence of Mn<sup>2+</sup>, and to a lesser degree in the combined presence of Mg<sup>2+</sup> and absence of Ca<sup>2+</sup>. PMA consistently increased KIM127 expression by a significant, but markedly lesser amount than Mn<sup>2+</sup>. The greater effect of Mn<sup>2+</sup> than PMA is consistent with induction of the m24 epitope by Mn<sup>2+</sup>, but not PMA (51); however, results with the KIM127 epitope differ in that PMA induces a small, but consistent increase in expression. We compared KIM127 with three other mAbs that were previously reported to activate cell adhesion mediated by  $\beta_2$  integrins (27–30). We found that mAbs KIM185, CBR LFA-1/2, and MEM48 bound equally well to wild-type and mutationally activated  $\alpha_L\beta_2$ , and activated ligand binding by wild-type  $\alpha_L\beta_2$  to a similar extent. By contrast, KIM127 bound to a much lower extent to wild-type  $\alpha_L\beta_2$ , yet activated ligand binding by wild-type  $\alpha_L\beta_2$  to the same extent. It is likely that KIM127 activates adhesion by binding to and stabilizing a complex between  $\alpha_L\beta_2$  and an ICAM. It is well known that many mAbs that appear specific for activated integrins bind to ligand-induced binding sites or LIBS (52).

Interesting differences were noted among the four activating mAbs in their ability to bind to  $\alpha_L\beta_2$ ,  $\alpha_M\beta_2$ , and  $\alpha_X\beta_2$ . For all three wild-type integrins, there was little expression of the KIM127 epitope, and the activating truncation of the  $\beta_2$  cytoplasmic domain induced full

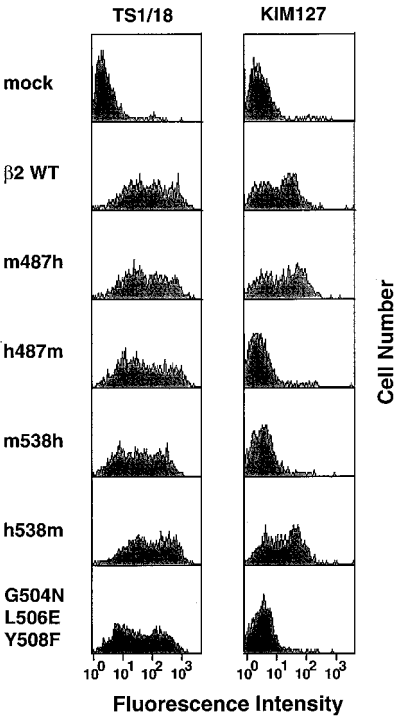
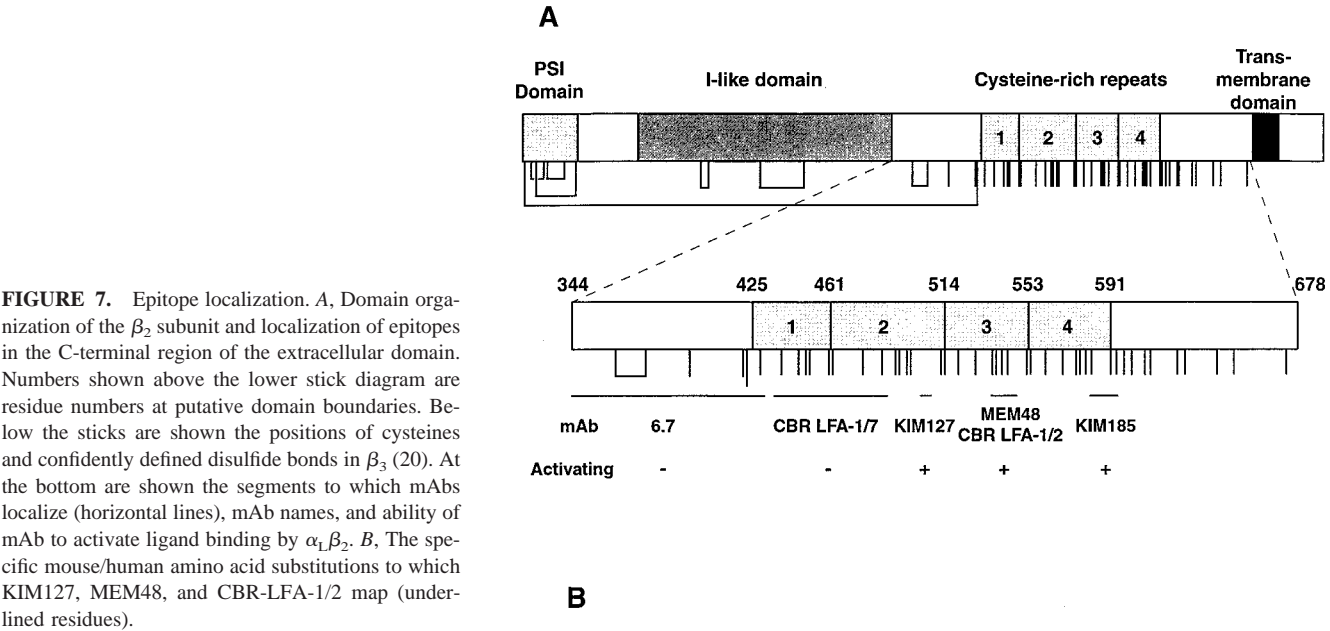


FIGURE 6. Mapping of KIM127 with immunofluorescent flow cytometry of 293T transfectants. The 293T cells were transiently cotransfected with  $\alpha_L$  in combination with wild-type  $\beta_2$  or human/mouse chimeric  $\beta_2$ , as indicated. As a control, the cells were transfected with vector alone (mock). The transfectants were stained with mAb TS1/18 to the I-like domain of the  $\beta_2$  subunit or mAb KIM127, then with FITC-conjugated anti-IgG, and subjected to immunofluorescent flow cytometry.



expression. However, wild-type  $\alpha_L\beta_2$ ,  $\alpha_M\beta_2$ , and  $\alpha_X\beta_2$  differed in expression of the MEM48, CBR LFA-1/2, and KIM185 epitopes. These three epitopes were all well expressed on wild-type  $\alpha_L\beta_2$ , but not on  $\alpha_M\beta_2$  and  $\alpha_X\beta_2$ . The KIM185 epitope was not well expressed on resting  $\alpha_M\beta_2$ , but was on resting  $\alpha_X\beta_2$ . CBR LFA-1/2 and MEM48 were more similar to one another in reactivity than to

KIM127 or KIM185, correlating with binding to overlapping epitopes. Both CBR LFA-1/2 and MEM48 mAbs bound to resting  $\alpha_L\beta_2$ , bound little to resting  $\alpha_X\beta_2$ , and showed intermediate reactivity with resting  $\alpha_M\beta_2$ , with MEM48 reacting better than CBR LFA-1/2. The activating truncation of the  $\beta_2$  cytoplasmic domain induced full expression of all four of these epitopes on  $\alpha_L\beta_2$ ,  $\alpha_M\beta_2$ , and  $\alpha_X\beta_2$ .

Table V. Fine mapping of mAb KIM127, MEM48, and CBR LFA-1/2 epitopes<sup>a</sup>

Human to mouse substitution	KIM127	MEM48	CBR LFA-1/2
V491I/L496V	+++++	+++++	+++++
G504N/L506E/Y508F	—	+++++	+++++
G504N	+	ND	ND
L506E	++++	ND	ND
Y508F	+++	ND	ND
T516N/I517V	+++++	+++++	+++++
G424S	+++++	+++++	+++++
P530S/G531D	+++++	+++++	+++++
L534S/F536N	+++++	—	—
L534S	ND	+	+++++
F536N	ND	+	++
R541S/H543K/F546Y	+++++	—	++
R541S	ND	+++++	+++++
H543K	ND	—	+++++
F546Y	ND	+++++	+++++
E554Q/T556S/E558T	+++++	+++++	+++++
P563A/R565L	+++++	+++++	+++++
R573H/R575Q/V578R	+++++	+++++	+++++
epitope	G504, L506, Y508	L534, F536, H543	L534, F536, R541, H543, F546

<sup>a</sup> Wild-type  $\beta_2$  or mutant  $\beta_2$  containing multiple or single human to mouse amino acid substitutions was coexpressed with the  $\alpha_L$  subunit in 293T cells, and mAb reactivity with the transfected cells was determined by flow cytometry. +++++, >90% of wild type; +++++, 70–90%; +++++, 50–70%; +++, 30–50%; +, <30%; —, no binding.



The differences between  $\alpha_L\beta_2$ ,  $\alpha_M\beta_2$ , and  $\alpha_X\beta_2$  in constitutive expression of the epitopes are interesting. Differences are consistent with our finding that the KIM127 epitope is shielded by the  $\alpha_L$  subunit in  $\beta_2$ , because the  $\alpha$  subunits differ in sequence and thus would be expected to differ in shielding. Differences in shielding could result both from subtle differences in conformation of the stalk regions of the  $\alpha$  subunits, and differences between the  $\alpha$  subunits in the way their stalk regions interact with the three different cysteine-rich repeats, to which these mAbs differentially map, repeats 2, 3, and 4.

Our studies provide a structure-function map for the C-terminal portion of the extracellular domain of the  $\beta_2$  subunit. Previously, little has been known about this segment, which appears to correspond to a stalk structure seen in electron micrographs of integrins. This region from residues 344 to 678 is often referred to as cysteine rich; however, the cysteine-rich repeats themselves correspond only to residues 425–591, and the regions from 344 to 425 and 591 to 678 have a lower cysteine content (Fig. 7). The segment from residues 344–678 contains 20 predicted  $\beta$ -strands and no predicted  $\alpha$ -helices, suggesting that it contains  $\beta$ -sandwich domains (16).

We have divided the  $\beta_2$  C-terminal region into five different mAb-defined segments, and show that the segment to which a mAb binds correlates with its ability to activate integrin adhesiveness (Fig. 7). The epitope of mAb 6.7 maps to residues 350–432, which correspond largely to the regions between the I-like domain and cysteine-rich repeat 1. mAb CBR LFA-1/7 maps largely to cysteine-rich repeat 1, and to a portion of cysteine-rich repeat 2 (residues 432–487). Neither of these Abs activates integrin adhesiveness. By contrast, all four mAbs that map to three more C-terminal segments that include cysteine-rich repeats 2, 3, and 4 activate  $\beta_2$  integrin adhesiveness. The binding sites for three of these mouse anti-human mAbs were narrowed down with individual human→mouse amino acid substitutions. KIM127 recognizes three residues, Gly<sup>504</sup>, Leu<sup>506</sup>, and Tyr<sup>508</sup>. These residues are located wholly within cysteine-rich repeat 2 (Fig. 7). mAbs MEM48 and CBR LFA-1/2 recognize overlapping epitopes located wholly within cysteine-rich repeat 3. mAb MEM48 recognizes residues Leu<sup>534</sup>, Phe<sup>536</sup>, and His<sup>543</sup>. mAb CBR LFA-1/2 recognizes residue Phe<sup>536</sup>, to a lesser extent residue Leu<sup>534</sup>, and a combination of two or more of the residues Arg<sup>541</sup>, His<sup>543</sup>, and Phe<sup>546</sup>. mAb KIM185 was mapped to residues 581–621. Together with a previous report localizing the C-terminal boundary of the KIM185 epitope to residue 604 (16), this shows that it recognizes a segment of 23 aa corresponding to the end of cysteine-rich repeat 4 and the beginning of the next region (Fig. 7). These results suggest that in particular cysteine-rich repeats 2 and 3, and possibly cysteine-rich repeat 4, are important in  $\beta_2$  integrin activation, whereas the more N-terminal regions of residues 344–432 and 432–487 have less or little function in  $\beta_2$  integrin activation.

For several reasons, we favor the interpretation that in resting integrins, there is an interaction of the  $\alpha$  subunit with cysteine-rich repeats 2 and 3 (and possibly 4) of the  $\beta_2$  subunit, and that upon activation this interface opens and becomes more exposed. Four disulfide bonds are present in each of these cysteine-rich repeats (20), and this suggests that these domains are rigid and unlikely to undergo any significant conformational change independently of interactions with the  $\alpha$  subunit. We found that all of the epitopes are present on the isolated  $\beta_2$  subunit, whereas exposure of the KIM127 epitope is greatly reduced in the  $\alpha_L\beta_2$ ,  $\alpha_M\beta_2$ , and  $\alpha_X\beta_2$  complexes. Furthermore, exposure of the CBR LFA-1/2, MEM48, and KIM185 epitopes is greatly reduced in either or both of  $\alpha_M\beta_2$  and  $\alpha_X\beta_2$ . Other studies suggest that interactions in integrin  $\beta$  subunit stalk regions restrain integrins in an inactive state, and that there is a loosening in this region upon activation. Species-specific substitutions in the  $\beta_2$  subunit activate ligand binding by  $\alpha_X\beta_2$ ,

and appear to define an interaction interface between the  $\alpha_X$  and  $\beta_2$  subunits that restrains  $\alpha_X\beta_2$  in an inactive conformation (53). These substitutions map to the PSI domain and cysteine-rich repeats 2 and 3, and the most activating substitutions were Gln<sup>525</sup>→Ser and Val<sup>526</sup>→Leu, in cysteine-rich repeat 3. These substitutions exposed the CBR LFA-1/2 epitope (53), which we also map within cysteine-rich repeat 3, to residues 534–546. In other studies, activation of  $\alpha_L\beta_2$  expressed on COS cells was induced if the C-terminal cysteine-rich-repeat region of the  $\beta_2$  subunit was replaced by that of  $\beta_1$  (54). A point mutation that introduces a *N*-glycosylation site into the beginning of cysteine-rich repeat 4 of the  $\beta_3$  subunit activates integrins  $\alpha_{IIb}\beta_3$  and  $\alpha_V\beta_3$  (55).

Several lines of evidence suggest that the epitopes in the  $\beta_2$  cysteine-rich repeats are shielded by the  $\alpha$  subunit and not some other associating molecule. First, the  $\alpha_L$ ,  $\alpha_M$ , and  $\alpha_X$  subunits differed in shielding of the CBR LFA-1/2, MEM48, and KIM185 epitopes. Second, in cell transfection experiments, these epitopes and the KIM127 epitope only became shielded when an  $\alpha$  subunit was cotransfected with the  $\beta_2$  subunit. Furthermore, no other associating molecules were seen in immunoprecipitation experiments, in which KIM127 mAb was found to immunoprecipitate the unassociated  $\beta_2$  subunit precursor well, but the  $\alpha_L\beta_2$  complex poorly (15).

Association between the  $\alpha$  and  $\beta$  subunit stalk regions and the  $\alpha$  and  $\beta$  subunit cytoplasmic/transmembrane domains may be linked. Previous work has suggested interactions between the  $\alpha$  and  $\beta$  subunit cytoplasmic/transmembrane domains that include complementary negatively and positively charged residues, and restrain integrins in an inactive state (56, 57). Consistent with this, mutations that activate  $\beta_2$  integrins, such as truncation of the  $\alpha_L$  or  $\beta_2$  cytoplasmic domains and removal of the GFFKR sequence, would disrupt  $\alpha$  and  $\beta$  subunit cytoplasmic/transmembrane interactions. We now show that these mutations also expose epitopes in cysteine-rich repeats 2 and 3, and near the end of cysteine-rich repeat 4. Our data suggest that these are important regulatory sites in the  $\beta_2$  subunit for  $\alpha_L\beta_2$  activation. We propose that in the resting integrin state (closed conformation), the C-terminal stalk-like regions of the  $\alpha$  and  $\beta_2$  subunits are kept close together by the transmembrane and cytoplasmic domains, and epitopes in cysteine-rich repeats 2, 3, and 4 are shielded by the  $\alpha$  subunit. We further propose that in the active state (open conformation), the release of the interactions between the  $\alpha$  and  $\beta$  subunit cytoplasmic/transmembrane domains results in a movement apart of the stalk-like regions of the  $\alpha$  and  $\beta$  subunits, thus exposing epitopes in cysteine-rich repeats 2, 3, and 4. The Abs to these epitopes may activate by acting like a wedge to keep the  $\alpha$  and  $\beta$  subunit stalk-like regions apart. The KIM127 epitope appears to be the most resistant to exposure, because it is shielded in all three resting  $\alpha\beta_2$  complexes that we examined. Interestingly, binding of the KIM185 mAb to a site that we map near the end of cysteine-rich repeat 4 can expose the KIM127 epitope, which we map to cysteine-rich repeat 2 (28). The opening of the stalk region may in turn alter the relative orientations of the  $\alpha$  and  $\beta$  subunits in the ligand-binding integrin headpiece. Conformational shifts around the MIDAS in I domains regulate ligand binding, and are linked to a large movement of the C-terminal  $\alpha$ -helix of the I domain that connects to other integrin domains (8–12). It appears that an alteration in contacts in the stalk region between the cysteine-rich repeats in the  $\beta$  subunit and the  $\alpha$  subunit is linked to conformational rearrangements in the ligand-binding domains in the headpiece of integrins. Our data provide new insights into the molecular mechanisms for integrin activation.

## References

1. Springer, T. A. 1990. Adhesion receptors of the immune system. *Nature* 346:425.
2. Springer, T. A. 1994. Traffic signals for lymphocyte recirculation and leukocyte emigration: the multi-step paradigm. *Cell* 76:301.



3. Gahmberg, C. G., M. Tolvanen, and P. Kotovuori. 1997. Leukocyte adhesion: structure and function of human leukocyte  $\beta_2$ -integrins and their cellular ligands. *Eur. J. Biochem.* 245:215.
4. Weisel, J. W., C. Nagaswami, G. Vilaire, and J. S. Bennett. 1992. Examination of the platelet membrane glycoprotein IIb-IIIa complex and its interaction with fibrinogen and other ligands by electron microscopy. *J. Biol. Chem.* 267:16637.
5. Springer, T. A. 1997. Folding of the N-terminal, ligand-binding region of integrin  $\alpha$ -subunits into a  $\beta$ -propeller domain. *Proc. Natl. Acad. Sci. USA* 94:65.
6. Springer, T. A., H. Jing, and J. Takagi. 2000. A novel  $\text{Ca}^{2+}$ -binding  $\beta$ -hairpin loop better resembles integrin sequence motifs than the EF-hand. *Cell* 102:275.
7. Lee, J.-O., P. Rieu, M. A. Arnaout, and R. Liddington. 1995. Crystal structure of the A domain from the  $\alpha$  subunit of integrin CR3 (CD11b/CD18). *Cell* 80:631.
8. Emsley, J., C. G. Knight, R. W. Farndale, M. J. Barnes, and R. C. Liddington. 2000. Structural basis of collagen recognition by integrin  $\alpha_2\beta_1$ . *Cell* 101:47.
9. Lee, J.-O., L. A. Bankston, M. A. Arnaout, and R. C. Liddington. 1995. Two conformations of the integrin A-domain (I-domain): a pathway for activation? *Structure* 3:1333.
10. Oxvig, C., C. Lu, and T. A. Springer. 1999. Conformational changes in tertiary structure near the ligand binding site of an integrin I domain. *Proc. Natl. Acad. Sci. USA* 96:2215.
11. Li, R., P. Rieu, D. L. Griffith, D. Scott, and M. A. Arnaout. 1998. Two functional states of the CD11b A-domain: correlations with key features of two  $\text{Mn}^{2+}$ -complexed crystal structures. *J. Cell Biol.* 143:1523.
12. Shimaoka, M., J. M. Shifman, H. Jing, J. Takagi, S. L. Mayo, and T. A. Springer. 2000. Computational design of an integrin I domain stabilized in the open, high affinity conformation. *Nat. Struct. Biol.* 7:674.
13. Tozer, E. C., R. C. Liddington, M. J. Sutcliffe, A. H. Smeeton, and J. C. Loftus. 1996. Ligand binding to integrin  $\alpha_{\text{IIb}}\beta_3$  is dependent on a MIDAS-like domain in the  $\beta_3$  subunit. *J. Biol. Chem.* 271:21978.
14. Tuckwell, D. S., and M. J. Humphries. 1997. A structure prediction for the ligand-binding region of the integrin  $\beta$  subunit: evidence for the presence of a von Willebrand factor A domain. *FEBS Lett.* 400:297.
15. Huang, C., C. Lu, and T. A. Springer. 1997. Folding of the conserved domain but not of flanking regions in the integrin  $\beta_2$  subunit requires association with the  $\alpha$  subunit. *Proc. Natl. Acad. Sci. USA* 94:3156.
16. Huang, C., Q. Zang, J. Takagi, and T. A. Springer. 2000. Structural and functional studies with antibodies to the integrin  $\beta_2$  subunit: a model for the I-like domain. *J. Biol. Chem.* 275:21514.
17. Puzon-McLaughlin, W., T. Kamata, and Y. Takada. 2000. Multiple discontinuous ligand-mimetic antibody binding sites define a ligand binding pocket in integrin  $\alpha_{\text{IIb}}\beta_3$ . *J. Biol. Chem.* 275:7795.
18. Zang, Q., C. Lu, C. Huang, J. Takagi, and T. A. Springer. 2000. The top of the I-like domain of the integrin LFA-1  $\beta$  subunit contacts the  $\alpha$  subunit  $\beta$ -propeller domain near  $\beta$ -sheet 3. *J. Biol. Chem.* 275:22202.
19. Lu, C., C. Oxvig, and T. A. Springer. 1998. The structure of the  $\beta$ -propeller domain and C-terminal region of the integrin  $\alpha_{\text{IIb}}\beta_3$  subunit. *J. Biol. Chem.* 273:15138.
20. Calvete, J. J., A. Henschen, and J. González-Rodríguez. 1991. Assignment of disulphide bonds in human platelet GPIIb: a disulphide pattern for the  $\beta$ -subunits of the integrin family. *Biochem. J.* 274:63.
21. Bork, P., T. Doerks, T. A. Springer, and B. Snel. 1999. Domains in plexins: links to integrins and transcription factors. *Trends Biochem. Sci.* 24:261.
22. Du, X., M. Gu, J. W. Weisel, C. Nagaswami, J. S. Bennett, R. Bowditch, and M. H. Ginsberg. 1993. Long range propagation of conformational changes in integrin  $\alpha_{\text{IIb}}\beta_3$ . *J. Biol. Chem.* 268:23087.
23. Shih, D. T., J. M. Edelman, A. F. Horwitz, G. B. Grunwald, and C. A. Buck. 1993. Structure/function analysis of the integrin  $\beta_1$  subunit by epitope mapping. *J. Cell Biol.* 122:1361.
24. Faull, R. J., J. Wang, D. I. Leavesley, W. Puzon, G. R. Russ, D. Vestweber, and Y. Takada. 1996. A novel activating anti- $\beta_1$  integrin monoclonal antibody binds to the cysteine-rich repeats in the  $\beta_1$  chain. *J. Biol. Chem.* 271:25099.
25. Bazzoni, G., D.-T. Shih, C. A. Buck, and M. A. Hemler. 1995. Monoclonal antibody 9EG7 defines a novel  $\beta_1$  integrin epitope induced by soluble ligand and manganese, but inhibited by calcium. *J. Biol. Chem.* 270:25570.
26. Takagi, J., T. Isobe, Y. Takada, and Y. Saito. 1997. Structural interlock between ligand-binding site and stalk-like region of  $\beta_1$  integrin revealed by a monoclonal antibody recognizing conformation-dependent epitope. *J. Biochem.* 121:914.
27. Robinson, M. K., D. Andrew, H. Rosen, D. Brown, S. Ortlepp, P. Stephens, and E. C. Butcher. 1992. Antibody against the Leu-cam  $\beta$ -chain (CD18) promotes both LFA-1- and CR3-dependent adhesion events. *J. Immunol.* 148:1080.
28. Andrew, D., A. Shock, E. Ball, S. Ortlepp, J. Bell, and M. Robinson. 1993. KIM185, a monoclonal antibody to CD18 which induces a change in the conformation of CD18 and promotes both LFA-1- and CR3-dependent adhesion. *Eur. J. Immunol.* 23:2217.
29. Binnerts, M. E., Y. van Kooyk, D. L. Simmons, and C. G. Figdor. 1994. Distinct binding of T lymphocytes to ICAM-1, -2 or -3 upon activation of LFA-1. *Eur. J. Immunol.* 24:2155.
30. Petruzzelli, L., L. Maduzia, and T. A. Springer. 1995. Activation of LFA-1 (CD11a/CD18) and Mac-1 (CD11b/CD18) mimicked by an antibody directed against CD18. *J. Immunol.* 155:854.
31. Stephens, P., J. T. Romer, M. Spitali, A. Shock, S. Ortlepp, C. Figdor, and M. K. Robinson. 1995. KIM127, an antibody that promotes adhesion, maps to a region of CD18 that includes cysteine-rich repeats. *Cell Adhes. Commun.* 3:375.
32. Sanchez-Madrid, F., A. M. Krensky, C. F. Ware, E. Robbins, J. L. Strominger, S. J. Burakoff, and T. A. Springer. 1982. Three distinct antigens associated with human T lymphocyte-mediated cytotoxicity: LFA-1, LFA-2, and LFA-3. *Proc. Natl. Acad. Sci. USA* 79:7489.
33. Bazil, V., I. Stefanova, I. Hilgert, H. Kristofova, S. Vanek, and V. Horejsi. 1990. Monoclonal antibodies against human leucocyte antigens. IV. Antibodies against subunits of the LFA-1 (CD11a/CD18) leukocyte-adhesion glycoprotein. *Folia Biol.* 36:41.
34. Pope, I., G. Hale, and H. Waldmann. 1989. Epitope mapping of rat CD11a/CD18 antibodies and comparison with third and fourth workshop panels. In *Leukocyte Typing IV*. W. Knapp, B. Dorken, W. R. Gilks, E. P. Rieber, R. E. Schmidt, H. Stein, and A. E. G. K. von dem Borne, eds. Oxford University Press, Oxford, p. 559.
35. David, V., G. Leca, N. Corvaia, F. Le Deist, L. Boumsell, and A. Bensussan. 1991. Proliferation of resting lymphocytes is induced by triggering T cells through an epitope common to the three CD18/CD11 leukocyte adhesion molecules. *Cell. Immunol.* 136:519.
36. Pedrinaci, S., C. Huelin, M. Patarroyo, F. Ruiz-Cabello, and F. Garrido. 1989. Studies on CD11a and CD18 molecules with two new monoclonal antibodies: differential myelomonocytic antigen expression of PMA treated HL60 and U937 cell lines. *Hybridoma* 8:13.
37. Keizer, G. D., J. Borst, C. G. Figdor, H. Spits, F. Miedema, C. Terhorst, and J. E. de Vries. 1985. Biochemical and functional characteristics of the human leukocyte membrane antigen family LFA-1, Mo-1 and p150,95. *Eur. J. Immunol.* 15:1142.
38. Miedema, F., P. A. T. Tetteroo, W. G. Hesselink, G. Werner, H. Spits, and C. J. M. Melief. 1984. Both Fc receptors and LFA-1 on human T  $\gamma$  lymphocytes are required for antibody-dependent cellular cytotoxicity (killer cell activity). *Eur. J. Immunol.* 14:518.
39. Lu, C., and T. A. Springer. 1997. The  $\alpha$  subunit cytoplasmic domain regulates the assembly and adhesiveness of integrin lymphocyte function-associated antigen-1 (LFA-1). *J. Immunol.* 159:268.
40. Seed, B., and A. Aruffo. 1987. Molecular cloning of the CD2 antigen, the T-cell erythrocyte receptor, by a rapid immunoselection procedure. *Proc. Natl. Acad. Sci. USA* 84:3365.
41. Ho, S. N., H. D. Hunt, R. M. Horton, J. K. Pullen, and L. R. Pease. 1989. Site-directed mutagenesis by overlap extension using the polymerase chain reaction. *Gene* 77:51.
42. Horton, R. M., Z. Cai, S. N. Ho, and L. R. Pease. 1990. Gene splicing by overlap extension: tailor-made genes using the polymerase chain reaction. *BioTechniques* 8:528.
43. DuBridge, R. B., P. Tang, H. C. Hsia, P. M. Leong, J. H. Miller, and M. P. Calos. 1987. Analysis of mutation in human cells by using an Epstein-Barr virus shuttle system. *Mol. Cell. Biol.* 7:379.
44. Heinzel, S. S., P. J. Krysan, M. P. Calos, and R. B. DuBridge. 1988. Use of simian virus 40 replication to amplify Epstein-Barr virus shuttle vectors in human cells. *J. Virol.* 62:3738.
45. Dransfield, I., and N. Hogg. 1989. Regulated expression of  $\text{Mg}^{2+}$  binding epitope on leukocyte integrin  $\alpha$  subunits. *EMBO J.* 8:3759.
46. Lub, M., S. J. van Vliet, S. P. Oomen, R. A. Pieters, M. Robinson, C. G. Figdor, and Y. van Kooyk. 1997. Cytoplasmic tails of  $\beta_1$ ,  $\beta_2$ , and  $\beta_3$  integrins differentially regulate LFA-1 function in K562 cells. *Mol. Biol. Cell* 8:719.
47. Larson, R. S., M. L. Hibbs, A. L. Corbi, E. Luther, J. Garcia-Aguilar, and T. A. Springer. 1989. The subunit specificity of the CD11a/CD18, CD11b, and CD11c panels of antibodies. In *Leukocyte Typing IV*. W. Knapp, B. Dorken, W. R. Gilks, E. P. Rieber, R. E. Schmidt, H. Stein, and A. E. G. K. von dem Borne, eds. Oxford University, London, p. 566.
48. Dransfield, I., C. Cabañas, A. Craig, and N. Hogg. 1992. Divalent cation regulation of the function of the leukocyte integrin LFA-1. *J. Cell Biol.* 116:219.
49. Rothlein, R., and T. A. Springer. 1986. The requirement for lymphocyte function-associated antigen 1 in homotypic leukocyte adhesion stimulated by phorbol ester. *J. Exp. Med.* 163:1132.
50. Dustin, M. L., and T. A. Springer. 1989. T cell receptor cross-linking transiently stimulates adhesiveness through LFA-1. *Nature* 341:619.
51. Stewart, M. P., C. Cabañas, and N. Hogg. 1996. T cell adhesion to intercellular adhesion molecule-1 (ICAM-1) is controlled by cell spreading and the activation of integrin LFA-1. *J. Immunol.* 156:1810.
52. Bazzoni, G., and M. E. Hemler. 1998. Are changes in integrin affinity and conformation overemphasized? *Trends Biochem. Sci.* 23:30.
53. Zang, Q., and T. A. Springer. 2000. Amino acid residues in the PSI domain and cysteine-rich repeats of the integrin  $\beta_2$  subunit that restrain activation of the integrin  $\alpha_X\beta_2$ . *J. Biol. Chem.* 276:6922.
54. Douglass, W. A., R. H. Hyland, C. D. Buckley, A. Al-Shamkhani, J. M. Shaw, S. L. Scarth, D. L. Simmons, and S. K. A. Law. 1998. The role of the cysteine-rich region of the  $\beta_2$  integrin subunit in the leukocyte function-associated antigen-1 (LFA-1,  $\alpha_L\beta_2$ , CD11a/CD18) heterodimer formation and ligand binding. *FEBS Lett.* 440:414.
55. Kashiwagi, H., Y. Tomiyama, S. Tadokoro, S. Honda, M. Shiraga, H. Mizutani, M. Handa, Y. Kurata, Y. Matsuzawa, and S. J. Shattil. 1999. A mutation in the extracellular cysteine-rich repeat region of the  $\beta_3$  subunit activates integrins  $\alpha_{\text{IIb}}\beta_3$  and  $\alpha_v\beta_3$ . *Blood* 93:2559.
56. Hughes, P. E., F. Diaz-Gonzalez, L. Leong, C. Wu, J. A. McDonald, S. J. Shattil, and M. H. Ginsberg. 1996. Breaking the integrin hinge. *J. Biol. Chem.* 271:6571.
57. O'Toole, T. E., Y. Katagiri, R. J. Faull, K. Peter, R. Tamura, V. Quaranta, J. C. Loftus, S. J. Shattil, and M. H. Ginsberg. 1994. Integrin cytoplasmic domains mediate inside-out signal transduction. *J. Cell Biol.* 124:1047.
58. Lu, C., M. Shimaoka, Q. Zang, J. Takagi, and T. A. Springer. 2001. Locking in alternate conformations of the integrin  $\alpha_L\beta_2$  I domain with disulfide bonds reveals functional relationships among integrin domains. *Proc. Natl. Acad. Sci. USA* 98:2393.